

Extreme precipitation events and the applicability of Global Climate Models to the study of floods and droughts

Z. Kothavala and A. Henderson-Sellers

Climatic Impacts Centre, Macquarie University, Sydney, Australia

Abstract While current validation techniques of General Circulation Model (GCM) output are primarily associated with the examination of the average of climate variables at seasonal and monthly scales, there has been little research on the evaluation of climate model results at the daily time scale. A detailed study of daily precipitation of present day and enhanced greenhouse simulations from five atmospheric GCMs, conducted under the auspices of the Model Evaluation Consortium for Climate Assessment (MECCA) project, show that the intensification of the hydrologic cycle simulated by all GCMs under enhanced levels of greenhouse gases is attributed to an increase in the frequency of heavy precipitation events. Most models reproduce the zonal frequency of extreme precipitation reasonably well over land. In IPCC Region 1 (midwest USA), an increase in the mean precipitation is accompanied by a concomitant increase in the variability and a decrease in the number of raindays-per-year. The ninetieth percentile of daily rainfall increases. The return period of heavy rainfall events decreases. The Palmer Drought Severity Index (PDSI) is used to determine whether the changes in rainfall regimes may lead to more floods or droughts. Application of the PDSI, using precipitation and temperature from a 10-year equilibrated simulation generated by one of the MECCA models for a typical grid point in midwest USA, shows that instances of dry and wet-spells, occur more frequently under enhanced greenhouse conditions.

KEY WORDS: Daily precipitation, General Circulation Models, Palmer Drought Severity Index

1. Introduction

The anticipated increase in global temperatures caused by increasing levels of anthropogenically induced greenhouse gases is likely to be an important factor in the distribution of water resources in future climates. The absorption of longwave radiation by greenhouse gases is expected to cause an increase in global temperatures. A warmer atmosphere is capable of holding more moisture because of the exponential relationship between temperature and water vapour (described by the *Clausius-Clapeyron equation*). The increase in temperature, causes an increase in evaporation and a consequent increase in precipitation. The plausible impacts of increased precipitation are greater instances of increased wet spells with the possibility of floods. Prior research by Manabe *et al.* (1981)[8] suggests the possible occurrence of mid-latitude summer time droughts.

This, and other heightened concerns over the possible impact of future climate changes, lead to the creation of the Model Evaluation Consortium for Climate Assessment (MECCA)¹ project (Henderson-Sellers *et al.* 1995 [5]) in 1991 with the following goals:

- To perform numerical experiments that will identify and quantify the uncertainties associated with predictions of greenhouse gas-induced climate change for models used to advise public policy;
- To create a protocol for analysing the experimental results and applying them to policy; and

¹The project Policy and Technical Committee decreed on April 20, 1995 to change the acronym to MECCA.

- To communicate findings in order to advance model development.

General Circulation Models (GCMs) are widely regarded as the "most acceptable tool" to study climate change (Houghton *et al.* 1990) [6]. GCMs have five basic variables: *viz.* temperature (determined by the Thermodynamic equation); humidity and surface pressure (determined by equations for the conservation of water substances and mass); and, the north-south and east-west wind components (determined by the Navier-Stokes equation). Values of these variables are prognostically derived at various levels. The above equations may be solved using finite differences or spectral techniques. This physical and mathematical representation of atmospheric processes such as clouds, precipitation, radiative heating and surface friction, that occur at small scales over a typical GCM grid box is called parameterization. Atmospheric GCMs can be regarded as Numerical Weather Prediction (NWP) models which have been adapted for running over long periods of time (generally decades) by prescribing sea-surface temperatures from climatological data, and by varying the solar zenith angle by day and season (Mitchell, 1989)[9].

This paper examines the present day and enhanced greenhouse gas simulations of precipitation in GCMs. Section 2 briefly discusses the ability of GCMs in simulating extreme precipitation events. The combined effect of precipitation and temperature for a grid point in IPCC Region 1 (midwest USA)(105°-80°W, 35°-50°N) is examined to determine the probability of the occurrence of floods and/or droughts under enhanced CO₂ conditions using a

drought index in Section 3. The applicability of GCMs to the study of floods and droughts using this technique is discussed in section 4.

2. Extreme Events

Current validation techniques of GCM output are primarily associated with the examination of the *average* of many climate variables. While the use of averages may be acceptable to validate precipitation and temperature from Global Climate Models at seasonal and monthly scales (Rowntree *et al.* 1993 [12]; Mitchell, 1989[9]), the validation of daily data requires an examination of the frequency and magnitude of extreme events. Changes in extreme precipitation events, in particular, have received limited attention in the literature (Gordon *et al.* 1992[4], Rind *et al.* 1989[11]) despite their potential impact (Wigley, 1985) [15]. The use of daily GCM output for impact analysis requires adequate validation of most variables at the diurnal scale. It is often argued that in such cases, the variability is more important than the mean (e.g., Katz and Brown 1992)[7].

Zonal Precipitation over land

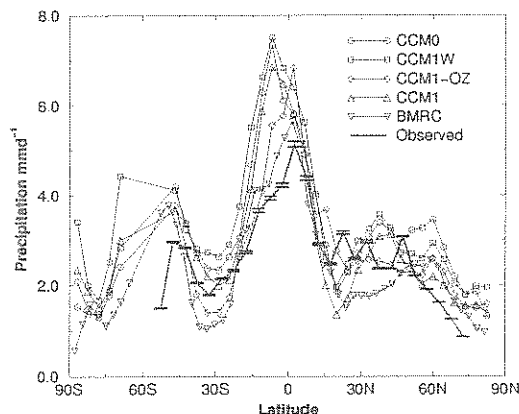


Figure 1: Zonally averaged precipitation for all models over land. The dotted line represents mean precipitation using station data at each 5° latitude band. The error bars represent two standard errors to account for differing number of stations averaged.

Four of the five GCMs (shown in Figure 1) are various configurations of the NCAR Community Climate Modelling group and the fifth is from the Bureau of Meteorology Research Centre (BMRC). CCM1-OZ is the model presented as an example in this paper. CCM1-OZ has a R15 horizontal resolution with twelve vertical layers, is coupled to the BATS land-surface scheme and incorporates a seasonal and diurnal cycle. The model incorporates a Q flux correction, includes a convective scheme based on moist convective adjustment, has a mixed layer ocean and three layers of sea-ice. Details of the history and parameterisation of other GCMs are not discussed in this paper. Nevertheless, it should be noted that all the GCMs analysed in this paper have mixed layer oceans and will not display the inter-seasonal and inter-annual variability of GCMs coupled to a full 3-D ocean - a factor that

is important to the study of droughts.

Probability of precipitation greater than 40 mm/day

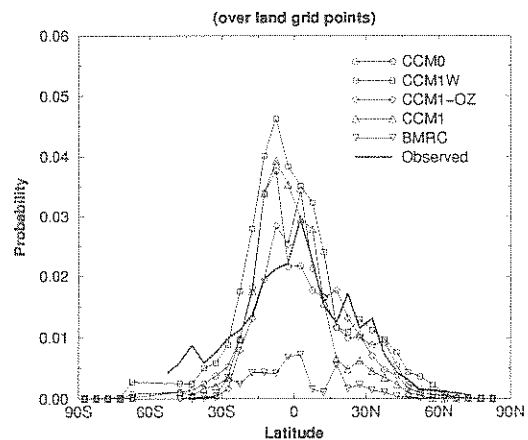


Figure 2: Zonally averaged probability of precipitation greater than 40 mm d^{-1} over land. The dotted line shows the probability of extreme precipitation from station data at every 5° latitude band from 1981-90.

The coarse resolution of these GCMs, means that precipitation processes are parameterised over a grid box with sides a few hundred kilometres in length. Since convective processes occur over much smaller spatial scales, the study of heavy rainfall events using GCMs is at best qualitative (Fowler and Hennessy, 1995[3]; Gordon *et al.* 1992[4]). The validation of the frequency of such events with observed data is a step towards the quantification of uncertainty arising from climate model parameterizations. Until now, this has not been attempted at the global scale due to the volume of information required and other caveats associated with comparing point with grid area information. The first step in this process is to ensure that the models capture the current day-to-day variability of climate in their control simulations.

Most models reproduce the zonal average precipitation reasonably well over land (see Figure 1) with differences in their capability to simulate the probability of heavy rainfall (see Figure 2). In IPCC Region 1, an increase in the mean precipitation is accompanied by a concomitant increase in the standard deviation i.e., the variability (see Table 1). The number of raindays-per-year decreases resulting in an increase in intensity (rain-per-rainday) to account for the increase in average rainfall. The intensification of the hydrologic cycle expected under enhanced greenhouse conditions is reflected in the increase in the ninetieth percentile value of average rainfall over the region. The model showed that the maximum precipitation occurred during the northern hemisphere summer months and the minimum precipitation in November. This did not change under enhanced greenhouse conditions because of the models incorporation of the seasonal cycle and a mixed layer ocean.

The return period (defined as that amount of area-averaged precipitation equalled or exceeded within a certain time frame) of heavy rainfall events decreases within

Table 1: Descriptive statistics for midwest USA

	CCM1-OZ	
	1×CO ₂	2×CO ₂
mean precipitation (mmd ⁻¹)	2.52	2.59
standard deviation (mmd ⁻¹)	2.69	2.88
raindays-per-year	207	200
rain-per-rainday (mmd ⁻¹)	7.79	8.52
month with max. precipitation	Aug	Jul
max. precipitation (mm/month)	180.85	171.93
month with min. precipitation	Nov	Nov
min. precipitation (mm/month)	20.21	21.84
10 th percentile (mmd ⁻¹)	0.41	0.39
90 th percentile (mmd ⁻¹)	5.80	6.07

the 10 year period of control and enhanced CO₂ simulations (see Figure 3). The five year event in the control simulation of CCM1-OZ over midwest USA, becomes a one-year event under enhanced CO₂ conditions. The one year event in the control simulation becomes a six month event, occurring twice as often under enhanced CO₂ conditions. These results showing an increase in rainfall intensity, a decrease in the number of raindays and a decrease in the return periods of heavy rainfall concur with earlier findings of Gordon *et al.* (1992) and Fowler and Hennessy (1995)[3] using different GCMs. Assuming that these changes in the magnitude and frequency of heavy precipitation events simulated by different GCMs are realistic, their impacts on the likelihood of greater floods and prolonged dry spells require further research. This, is the focus of the following section.

3. The Palmer Drought Severity Index

The Palmer Drought Severity Index (PDSI) developed by Palmer (1965) [10], operates on a monthly time series of precipitation and temperature to produce a single numerical value between +6 and -6 to represent the severity of wetness or aridity for a particular month (see Table 2). The index takes into consideration precipitation, potential evapotranspiration, antecedent soil moisture and runoff. Palmer evaluated drought in such a way that his index measures departures from appropriate values of precipitation. Persistently normal temperature and precipitation produce an index of zero in all seasons in all climates.

The Palmer Index has been widely used in the USA, Australia (Smith *et al.* 1994)[13] and in some other areas of the world (e.g., Briffa *et al.* 1994)[2]. The following description is based largely on descriptions given in Palmer (1965)[10] and Briffa *et al.* (1994)[2]. Palmer originally envisaged the use of monthly mean precipitation (P) and temperature data to calculate the monthly water balance in a simple two-layer soil model. Initially, several local coefficients are calculated which define local hydrological normals related to temperature and precipitation averaged over some calibration period. These coefficients ($\alpha, \beta, \gamma, \delta$) are calculated for individual months in each region as follows:

IPCC Region 1: Midwest USA

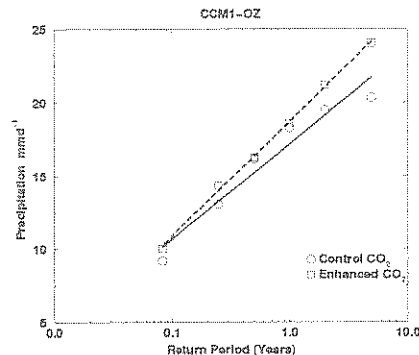


Figure 3: Return periods of extreme rainfall based on 10 years of equilibrium simulated daily rainfall using CCM1-OZ. Solid and dashed lines represent control and enhanced CO₂ simulations respectively.

$$\alpha = \overline{ET}/\overline{PE} \quad (1)$$

$$\beta = \overline{R}/\overline{PR} \quad (2)$$

$$\gamma = \overline{RO}/\overline{PRO} \quad (3)$$

$$\delta = \overline{L}/\overline{PL} \quad (4)$$

where PE is the potential evapotranspiration (calculated from the temperature data according to Thornthwaite, 1948[14]), ET the actual evapotranspiration, R the soil water recharge, PR the potential soil-water recharge, RO the runoff, PRO the potential runoff, L the water loss from the soil and PL the potential water loss from the soil. The overbars signify that these are the average quantities, derived using the appropriate month's data averaged over some calibration period.

The terms on the right hand side of the above equations satisfy the water balance equation

$$\hat{P} = \overline{ET} + \overline{R} + \overline{RO} + \overline{L} \quad (5)$$

where \hat{P} is the 'climatically appropriate for existing conditions' (CAFEC) value for precipitation.

Evapotranspiration losses from the soil occur when $PE > P$. Losses from the surface layer (L_s) are assumed to occur at the potential rate. Losses from the underlying layer (L_u) depend on the initial moisture content, PE , and the combined soil water content (SWC) in both layers. The upper layer is assumed to have a 25-mm water storage capacity. The available water capacity (AWC) of the underlying layer depends on local soil type. Moisture cannot be removed from or be replenished in, the underlying layer until the available moisture has been removed completely from, or replenished in, the surface layer. Hence

$$L_s = \min(S_s, PE - P) \quad (6)$$

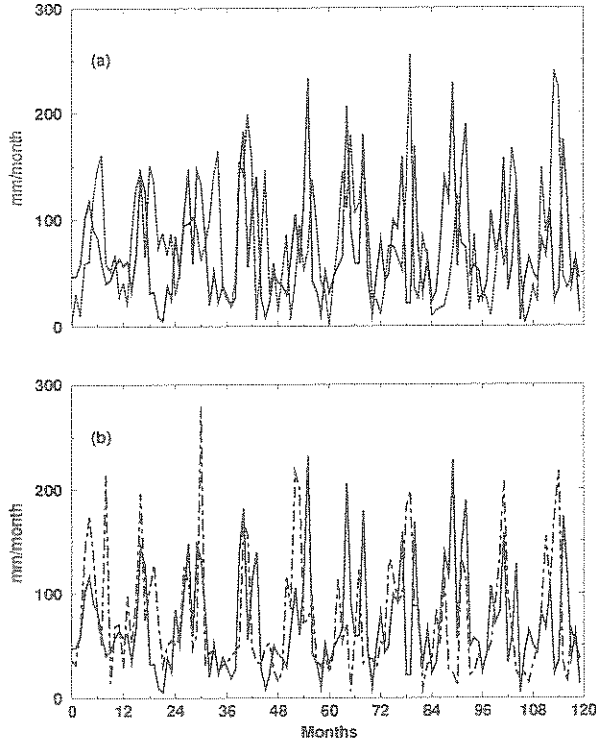


Figure 4: Monthly precipitation for Des Moines, Iowa: (a) CCM1-OZ control CO₂ simulation (solid line) Observed station data 1981-90 (dotted line); and (b) CCM1-OZ control CO₂ simulation (solid line) enhanced CO₂ simulation (dashed line)

and

$$L_u = [(PE - P) - L_s]S_u / AWC \quad (7)$$

where S_s and S_u are the initial moisture values in the surface and underlying layers at the beginning of the month. Runoff cannot occur unless both layers reach their combined capacity.

The potential terms (recharge, loss and runoff) are calculated as:

$$PR = AWC - (S_s + S_u) \quad (8)$$

$$PL = PL_s - PL_u \quad (9)$$

where

$$PL_s = \min(PE, S_s) \quad (10)$$

and

$$PL_u = (PE - PL_s)S_u / AWC \quad (11)$$

$$PRO = AWC - PR \quad (12)$$

Potential recharge (PR) is defined as the amount of moisture required to bring the soil water up to field capacity (i.e. AWC). Potential loss (PL) is the soil moisture that could be lost to evapotranspiration if precipitation

was zero for that month. Potential runoff (PRO) is defined as the potential precipitation (assumed by Palmer to be equal to the AWC) minus potential recharge. Given α , β , γ , δ , the PDSI calculation for a given month then commences by calculating a precipitation anomaly

$$d = P - \hat{P} \quad (13)$$

where $\hat{P} = \alpha PE + \beta PR + \gamma PRO + \delta PL$ (equivalent to equation 5). A moisture anomaly index (Z) is then calculated as

$$Z = Kd \quad (14)$$

where K is a weighting factor determined by Palmer (1965) from the calibration period data. Scaling d by K in effect standardizes the moisture anomaly by scaling it to a degree determined by local conditions. Palmer defined the scaling factor for a particular month as

$$K = \left(17.67 K' / \sum_{i=1}^{12} \bar{D} K' \right) K' \quad (15)$$

where \bar{D} is the mean of the absolute values of d for that month over all years in the calibration period, and

$$K' = 1.5 \log_{10} \{ [(\overline{PE} + \overline{R} + \overline{RO}) / \overline{P} + \overline{L}] + 2.8 \overline{D}^{-1} \} + 0.5 \quad (16)$$

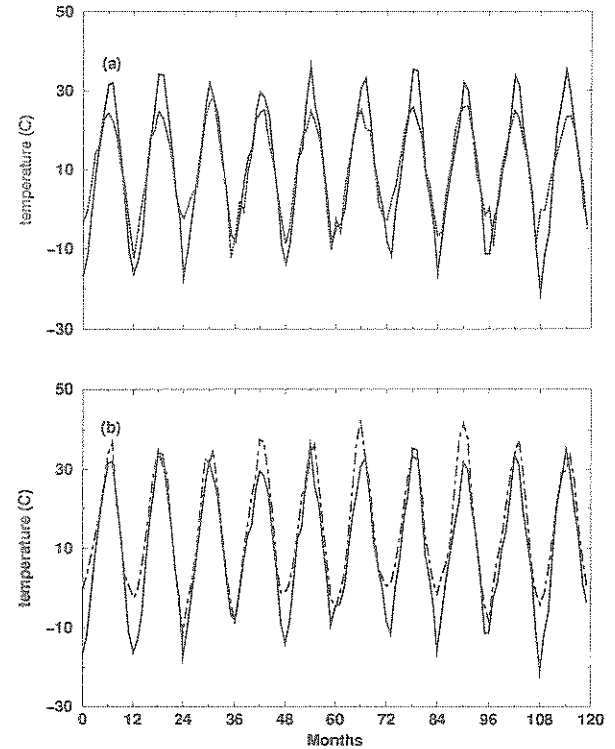


Figure 5: Monthly temperature for Des Moines, Iowa as in Figure 4

The summation in equation 15 denotes that the divisor is calculated as an annual value. The unit of calculation

Table 2: Description of monthly moisture conditions

Index	Characteristic	O	C	E
4.00 or more	Extremely wet	1	6	1
3.00 to 3.99	Very wet	2	2	13
2.00 to 2.99	Moderately wet	14	5	15
1.00 to 1.99	Slightly wet	12	19	13
0.99 to -0.99	Near normal	46	61	37
-1.00 to -1.99	Mild drought	15	14	13
-2.00 to -2.99	Moderate drought	9	7	21
-3.00 to -3.99	Severe drought	12	5	7
-4.00 or less	Extreme drought	0	1	0

in these equations is inches. The constants (17.62, 2.8 and 0.5) in equations 15 and 16 were derived by Palmer (1965) after much experimentation using annually aggregated data from only nine USA climate divisions. Their general applicability for scaling individual monthly Z values and, more particularly, when applied to climate data very different from those encompassed in Palmer's nine regions, must be open to question (Alley, 1984)[1]. However, these nine regions represent a wide range of climate conditions and many subsequent applications of the PDSI method in various regions of the USA have found it to be satisfactory.

Having calculated Z for a given month (i), the PDSI is given by

$$PDSI_i = PDSI_{(i-1)} + 0.33Z_i - 0.103PDSI_{(i-1)} \quad (17)$$

where the initial month, in a spell of dry or wet weather, is simply equal to $0.33 \times Z_i$. Equation 15 reduces to

$$PDSI_i = 0.897PDSI_{(i-1)} + 0.33Z_i \quad (18)$$

Palmer (1965) modified the procedure according to whether a dry or wet spell was already established. A spell is considered to have become established once the absolute value of the PDSI exceeds 1.0. The end of a dry spell does not necessarily indicate the start of a wet spell (and vice-versa). The beginning and ending of spells are determined by continually monitoring three PDSI series: (i) index for a wet spell becoming established (X_1); (ii) index for a dry spell becoming established (X_2); (iii) index for a wet or dry spell that is currently established (X_3).

X_1 is always positive and X_2 negative. When the value of X_3 reaches 1.0, it will equal either X_1 or X_2 depending on the sign. Droughts (and wet spells) end when X_3 returns to a value within the range ± 0.5 (i.e. near normal). Rather than wait for a spell to end, for a particular (current) month (i), Palmer (1965) calculated a 'percentage probability' that the spell had ended according to

$$P_e = \sum_{j=0}^{j^*} U_{i-j} / \left(Z_e + \sum_{j=1}^{j^*} U_{i-j} \right) \times 100 \quad (19)$$

where j^* is the number of months before the current one (i) that a spell became established, and

$$Z_e = -2.691X_{3(i-1)} \pm 1.5 \quad (20)$$

For wet spells, the sign in equation 20 is positive and for dry spells, it is negative. Variable U is equal to $Z_i \pm 0.15$. A dry or wet spell is deemed to have ended when P_e exceeds zero percent.

4. Application of the PDSI

It is generally preferable to compare the climate of one grid point to a set of stations equally distributed throughout the grid square. However, the area examined in this analysis is relatively free from high relief and has a homogeneous vegetation cover. Therefore, the climate measured at one station (Des Moines, Iowa (41.53°N, 93.65°W)), although it does not represent the climate of the full grid square, is used to demonstrate the ability of the index to capture extreme events in the 1981-90 time period. Precipitation and temperature from a typical grid point in IPCC Region 1 (midwest USA), using the control and enhanced greenhouse simulations of CCM1-OZ were applied to the PDSI. The nature of PDSI is such that the total of the monthly PDSI values should sum to zero. The sum of the 120 index values from the observations, the control and enhanced CO₂ simulations are -0.03, 0.11 and 0.08 respectively implying successful execution of the index.

The observed precipitation is somewhat similar in magnitude and seasonality, to precipitation simulated by the control run of the GCM (Figure 4(a)). The seasonal amplitude of monthly temperature of the station is greater than that of the control run of CCM1-OZ (Figure 5(a)). Nevertheless, the twelve month running mean of the control simulation of the GCM coincide with that of the observations for precipitation and temperature. Under enhanced greenhouse conditions, mean monthly precipitation for the grid point increases by 5.2%, the standard deviation increases by 13% and the seasonal range increases by 20.13% (Figure 4(b)). Mean monthly temperature increases by almost 5°C under enhanced greenhouse conditions however, there is a noticeable decrease in the seasonal temperature range of almost 3°C possibly due to higher minimum temperatures in the diurnal cycle of the GCM (Figure 5(b)).

The PDSI when forced with observed monthly average temperature and total accumulated monthly precipitation station data for Des Moines, Iowa from 1981-1990 (Figure 6(a)) reproduce the severe drought of 1988 during months 90-102. Frequent large amounts of precipitation are responsible for the prolonged wet-spells for months 84-96 in the control CO₂ simulation of the GCM (Figure 6(b)). Droughts are more prolonged under enhanced CO₂ conditions (Figure 6(c)) and tend to occur during the summer months primarily due to lower than normal precipitation in the preceding months (Figure 4(a)). Under enhanced CO₂ conditions, months classified as having moderate drought increases threefold from 7 to 21 and those of severe drought from 5 to 7 (Table 2). At the other end of the scale, months classified as being moderately wet increase threefold from 5 to 15 and those classified as very

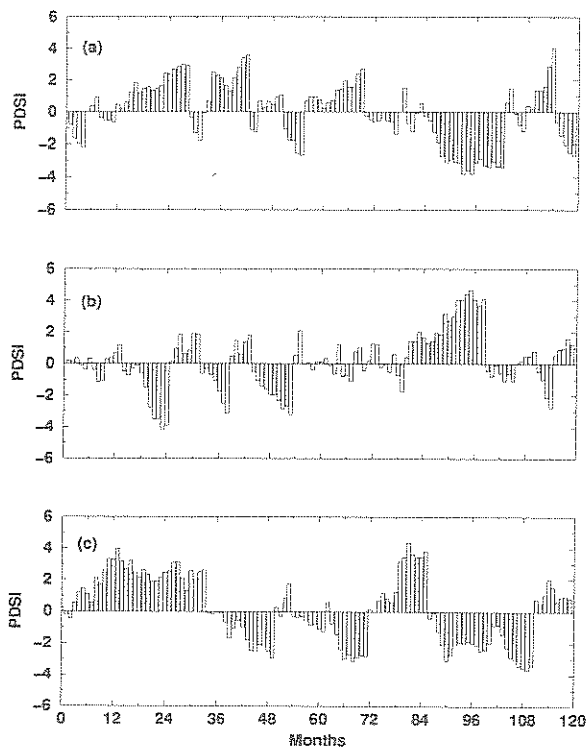


Figure 6: PDSI for Des Moines, Iowa (a) Station Observations 1981-90 (b) CCM1-OZ control CO₂ simulation (c) CCM1-OZ enhanced CO₂ simulation

wet increase from 2 to 13. There are also fewer months classified as near normal under enhanced greenhouse conditions in the ten year period analysed.

5. Conclusion

The model simulations suggest that the increase in mean precipitation over midwest USA, caused by the intensification of the hydrologic cycle under enhanced greenhouse conditions, is likely to cause an increase in the frequency of extreme rainfall events. It has been shown that this change in rainfall regimes over the study area will result in an increased incidence of wet spells and droughts. Extreme weather phenomena, such as flooding rains and droughts, are often related to the El Niño effect which is not simulated by GCMs that include a mixed layer ocean. The next stage of this research is the application of this technique to a GCM coupled to a 3-D ocean over a time scale spanning several decades.

Acknowledgements: This research is funded by the Model Evaluation Consortium of Climate Assessment (MECCA). Computational assistance was provided by J. Hoekstra from NV KEMA, The Netherlands. Station observations and the Palmer Drought Severity Index were acquired from the National Climate Data Center (NCDC) Asheville, NC. This is Contribution number 95/30 of the Climatic Impacts Centre.

References

- [1] W.M. Alley. The palmer drought severity index: Limitations and assumptions. *Journal of Climate and Applied Meteorology*, 23:1100-1109, 1984.
- [2] K.R. Briffa, P.D. Jones, and M. Hulme. Summer moisture availability across Europe,1892-1991: An analysis based on the Palmer drought severity index. *International Journal of Climatology*, 14:475-506, 1994.
- [3] A.M. Fowler and K.J. Hennessy. Potential impacts of global warming on the frequency and magnitude of heavy precipitation. *Natural Hazards*, 11(3):1-21, 1995.
- [4] H.B. Gordon, P.H. Whetton, A.B. Pittock, A.M. Fowler, and M.R. Haylock. Simulation changes in daily rainfall intensity due to the enhanced greenhouse effect: implications for extreme rainfall events. *Climate Dynamics*, 8:83-102, 1992.
- [5] A. Henderson-Sellers, W. Howe, and K. McGuffie. The MECCA analysis project. *Global and Planetary Change*, 10(1-4):3-21, 1995.
- [6] J.T. Houghton, G.J. Jenkins, and J.J. Ephraums. *Climate Change: The IPCC Scientific Assessment*. Cambridge University Press, 1990.
- [7] R.W. Katz and B.G. Brown. Extreme events in a changing climate: Variability is more important than averages. *Climatic Change*, 21:289-302, 1992.
- [8] S. Manabe. Summer dryness due to an increase in atmospheric CO₂ concentration. *Climatic Change*, 3:347-386, 1981.
- [9] J.F.B. Mitchell. The greenhouse effect and climate change. *Reviews of Geophysics*, 27:115-139, 1989.
- [10] W.C. Palmer. Meteorological drought. Technical Report 45, U.S. Weather Bureau, Washington, D.C., 1965.
- [11] D. Rind, R. Goldberg, and R. Ruedy. Change in climate variability in the 21st century. *Climatic Change*, 14:5-37, 1989.
- [12] P.R. Rowntree, J.M. Murphy, and J.F.B. Mitchell. Climatic change and future rainfall predictions. *J.IWEM*, 7:464-470, 1993.
- [13] D.I. Smith, M.F. Hutchinson, and R.J. McArthur. Climatic and agricultural drought: Payments and policy. Technical report, Centre for Resource and Environment Studies, ANU, Canberra, Australia, 1994.
- [14] C.W. Thornthwaite. An approach towards a rational classification of climate. *Geographical Review*, 38:55-94, 1948.
- [15] T.M.L. Wigley. Impacts of extreme events. *Nature*, 316(11):106-107, 1985.